

# Grand Canonical Monte Carlo Simulations of Hydrogen and Methane Storage Capacities of Two Novel Al-nia MOFs at Room Temperature

A. Granja-DelRío<sup>a</sup>, I. Cabria<sup>a,\*</sup>

<sup>a</sup>*Departamento de Física Teórica, Atómica y Óptica, Universidad de Valladolid, 47011 Valladolid, Spain*

---

## Abstract

Novel materials capable of storing hydrogen or/and methane at high gravimetric and volumetric densities are required for hydrogen vehicles to be widely employed as a clean alternative to fossil-based vehicles. Metal-Organic Frameworks (MOFs) are considered as promising candidates to achieve the Department Of Energy (DOE) targets for both, hydrogen and methane storage. Using Grand Canonical Monte Carlo (GCMC) simulations, the hydrogen and methane gravimetric and volumetric storage capacities of two recently synthesized Al-nia MOFs have been studied. Their storage capacities have been compared with the storage capacities of other Al-based MOFs and classical and well-known MOFs, such as IRMOF-5. The two novel Al-nia MOFs have shown high hydrogen and methane gravimetric and volumetric storage capacities at room temperature and moderate pressures, 25-35 MPa, comparable or higher than the storage capacities of classical and Al-based MOFs.

*Keywords:* Hydrogen Storage, Hydrogen Physisorption, Methane Storage, Al-based MOFs, Grand Canonical Monte Carlo Simulations

---

## 1. Introduction

Humankind evolution has led to important environmental threats and a major increase of energy consumption. Fuel combustion produces several harmful pollutants such as carbon dioxide or carbon monoxide. Adopting new strategies to replace fossil fuels could solve this

---

\*Corresponding author. Tel.: +34 983 423141; Fax: +34 983 423013

Email address: [ivan.cabria@uva.es](mailto:ivan.cabria@uva.es) (I. Cabria)

problem. Hydrogen is considered a very promising candidate to solve these issues. Basically, hydrogen reacts with atmospheric oxygen producing an electric current and emitting water. However, on-board hydrogen storage at room temperature and moderate pressures remains the principal obstacle to implement large fleets of fuel cell hydrogen vehicles [1]. Nowadays, hydrogen storage in vehicles is achieved by compressing gas at very high pressures. Decreasing these pressures will reduce the costs of these vehicles and refueling stations. The Department of Energy established two main targets for an on-board hydrogen storage system, to achieve before 2025: (a) a gravimetric capacity of at least 5.5 wt. % and (b) a volumetric capacity of at least 0.040 kg of hydrogen per liter [2, 3]. The goal of these targets is to obtain a hydrogen vehicle equivalent to the present average fossil fuel-based vehicle.

On the other hand, while the performance of hydrogen-powered vehicles is being improved, it might be necessary a transitional bridge between gasoline and hydrogen-based automobiles. Natural gas feels a good alternative since it is widely distributed, has huge reserves, low cost and is cleaner than oil. The reason is that the main component of natural gas, methane, has the highest ratio of hydrogen to carbon of all fossil fuels. Compared to coal, natural gas can reduce CO<sub>2</sub> emissions by 50 % [4]. Methane has higher gravimetric capacity than gasoline but, the challenge is to increase the volumetric density at ambient conditions. The main problem is, again, the storage. Natural gas is stored onboard the vehicle in compressed or liquefied form. These need expensive and bulky storage. The Advanced Research Projects Agency - Energy (ARPA-E) of the DOE set the targets for methane storage to lead the research on adsorbent materials for methane storage. The volumetric capacity needs to achieve 0.250 kg of methane/L and the gravimetric capacity 0.5 g/g or 33.33 wt. % at room temperature and moderate pressures [5].

Three main different types of hydrogen and methane storage have been proposed: liquid, compressed and solid. The last one includes the storage by physisorption on solid porous materials. That storage method allows storing more gas at low and moderate pressures ( $\leq$  25-35 MPa) than the compressed method [6, 7]. Development of efficient adsorbent solid porous materials is the key to achieve an efficient on-board storage technology. Many different porous materials have been evaluated as promising gas storage materials. Activated

carbons form a wide group of materials with a well-developed porosity, light weight and large hydrogen and methane storage capacities [8–11]. Covalent organic frameworks (COFs) represent another class of porous materials that are constructed through the covalent bonding of organic building blocks. COFs exhibit permanent porosity and possess tunable structures, making them highly appealing for gas storage applications [12–14]. Polymers of Intrinsic Microporosity (PIMs) possess a unique molecular structure that inherently incorporates microporosity, resulting in porous materials with remarkably high internal surface areas. This inherent characteristic grants PIMs the ability to display enhanced capacities for gas sorption [15–17].

In the last decades, many studies on adsorbed hydrogen and natural gas have focused on Metal-Organic Frameworks (MOFs), which are a group of promising solid porous materials for hydrogen and methane storage [18–24]. They are made of metal ions or metal containing clusters (secondary building blocks) linked by organic ligands to form 2D or 3D structures. The huge amount of organic linkers and the large variety of metal ions and metal clusters conduct to many different MOFs with tunable properties.

Recently, Alezi et al. [25] have synthesized two novel Al-nia MOFs which showed high porosity. Aluminum is an abundant element and hence, the synthesis of these MOFs is not expensive. Aluminum is also a light element and this implies, in general, high gravimetric storage capacities. The aims of this investigation are to predict and to study the hydrogen and methane storage capacities of these promising novel MOFs. Grand Canonical Monte Carlo (GCMC) simulations of the hydrogen and methane storage capacities of those two recently synthesized Al-nia-MOFs and of other MOFs have been performed. The storage capacities of these new materials have been compared with the capacities of other Al-based MOFs and of a set of classical and well-known MOFs. The storage capacities of all the MOFs simulated have been also analyzed as functions of the porosity and density of the MOFs.

## 2. Methodology

The GCMC simulations of the hydrogen and methane gravimetric and volumetric storage capacities of the two novel Al-nia-MOFs (Al-nia-MOF-1 and Al-nia-MOF-2), of a set of 15 Al-based MOFs, selected from the Cambridge Crystallographic Database Centre (CCDC) [26] and of a set of 21 classical MOFs have been performed at 298.15 K and pressures between 0.5 and 35 MPa. In addition, for Al-nia-MOF-1, CH<sub>4</sub> storage simulations at 298 K and 0.5 and 8 MPa were performed in order to compare the theoretical results with those from the experiment made by Alezi et al. [25].

The number of iterations in each GCMC simulation was ten millions. The first five millions were set to reach the equilibrium and the rest were employed to calculate the capacities. The Metropolis algorithm was used in each iteration [27]. The probabilities of the possible changes or moves were distributed as follows: 20 % consisted on the movement of one molecule, 40 % on the removal of one molecule and 40% for the addition of one molecule. The simulations were performed using an in-house code.

The chemical potential used in the simulations was obtained from the Soave-Redlich-Kwong (SRK) equation of state [28]. The values for the dimensionless acentric factor  $\omega$ , the critical pressure  $P_c$  and the critical temperature  $T_c$  of hydrogen and methane used in the SRK equation are those published by Zhou and Zhou [29] and Xu et al. [30], respectively.

Lennard-Jones (LJ) interaction potentials [31] have been used to simulate the interactions between the atoms of the MOFs and the molecules and between the molecules. The LJ coefficients used in the present simulations can be found in Table 1.

The LJ coefficients of the interaction between an atom and a molecule (hydrogen or methane) have been calculated using the Good-Hope [40] and the Berthelot [41] combining rules for the  $\sigma$  and  $\epsilon$  coefficients of the LJ potentials, respectively. In the case of the C-H<sub>2</sub> interaction, the LJ coefficients published by Rzepka et al. [38] have been used. The cutoff radius of the LJ interaction potential was 20 and 7.5 Å for the interactions with H<sub>2</sub> and methane, respectively. These values of the cutoff radii were obtained after carrying out several tests. To take into account the quantum effects, the Feynman-Hibbs [42] quantum

Table 1: Lennard-Jones coefficients  $\sigma$  and  $\epsilon$  of the molecules and of the atoms of the MOFs studied in the present GCMC simulations.

Atom or molecule	$\sigma(\text{\AA})$	$\epsilon(\text{eV})$	Source
Al	2.574	0.507220	Filippova et al. [32]
Br	3.519	0.016043	Mayo et al. [33]
C	3.400	0.003744	Tu et al. [34]
Cl	3.350	0.014951	Singer et al. [35]
Cu	2.297	0.520310	Filippova et al. [32]
H	2.846	0.000659	Mayo et al. [33]
N	3.310	0.003214	Cheung et al. [36]
O	3.033	0.004150	Mayo et al. [33]
S	3.590	0.014916	Mayo et al. [33]
Zn	0.998	0.008291	Soper et al. [37]
H <sub>2</sub>	2.970	0.002870	Rzepka et al. [38]
CH <sub>4</sub>	3.730	0.012748	Jorgensen et al. [39]
C-H <sub>2</sub>	3.190	0.002628	Rzepka et al. [38]

correction has been used.

In order to establish a comparison of interaction potentials, an alternative set of LJ coefficients, the MDT set, (MDT: Mayo, Darkrim and TraPPE) has been selected. This second set uses the LJ coefficients published by Mayo et al. [33] for the atoms, the LJ coefficients by Darkrim and Levesque [43] for the hydrogen molecule and the LJ coefficients of TraPPE [44] for methane. These coefficients can be found in Table 2.

### 2.1. Calculation of the Porosity

The porosity is the ratio of the available volume and the volume of the simulation cell of a MOF. This is a dimensionless magnitude. The difference between the volume of the simulation cell,  $V$ , and the volume occupied by the atoms of the MOF,  $V_{occ}$  is the available

Table 2: MDT set of Lennard-Jones coefficients  $\sigma$  and  $\epsilon$  of the molecules and of the atoms of the MOFs studied in the present GCMC simulations.

Atom or molecule	$\sigma(\text{\AA})$	$\epsilon(\text{eV})$	Source
Al	3.911	0.013442	Mayo et al. [33]
Br	3.519	0.016043	Mayo et al. [33]
C	3.473	0.004124	Mayo et al. [33]
Cl	3.519	0.012284	Mayo et al. [33]
Cu	3.093	0.002168	Mayo et al. [33]
H	2.846	0.000659	Mayo et al. [33]
N	3.263	0.003356	Mayo et al. [33]
O	3.033	0.004150	Mayo et al. [33]
S	3.590	0.014916	Mayo et al. [33]
Zn	4.045	0.002385	Mayo et al. [33]
H <sub>2</sub>	2.958	0.003163	Darkrim and Levesque [43]
CH <sub>4</sub>	3.730	0.012754	TraPPE [44]

volume to a gas molecule.

To calculate the volume  $V_{occ}$ , a grid of  $n$  points is created in the simulation cell. The volume  $V_{occ}$  is given by the  $Vni/n$ , where  $ni$  is the number of grid points that are inside the sphere of some atom of the simulation cell. The radius  $r$  of an atom is  $\sigma(atom, molecule)$  and the volume of the sphere of an atom is given by  $4\pi r^3/3$ . The LJ interaction potential energy is zero at an atom-molecule distance equal to  $\sigma(atom, molecule)$ . The available volume, the volume occupied by the atoms and the porosity depend on the type of gas molecule, due to this definition of the radius of an atom interacting with a molecule. The experimental porosity also depends on the type of gas.

## 2.2. Definitions of the Storage Capacities

The total (hydrogen or methane) volumetric storage capacity,  $v_c$ , also called the density of stored (hydrogen or methane), is defined in these simulations by

$$v_c = \frac{M_g}{V}, \quad (1)$$

where  $M_g$  is the mass of gas (hydrogen or methane) stored in the simulation cell and  $V$  is the volume of the simulation cell. Throughout this paper, the units of  $v_c$  are kg of H<sub>2</sub>/L or kg of CH<sub>4</sub>/L.

The total (hydrogen or methane) gravimetric storage capacity,  $g_c$ , is defined by

$$g_c = \frac{100M_g}{M_g + M_{ads}}, \quad (2)$$

where  $M_{ads}$  is the mass of the adsorbent solid porous material of the simulation cell. The units of the total gravimetric capacity are wt. %.

The usable, also called delivery or working, mass of gas (hydrogen or methane) stored at a  $P$  and  $T$  is the difference between the total mass of gas stored at  $P$  and  $T$  and the total mass of gas stored at the depletion pressure and  $T$  [2, 3, 45, 46]. The usable (hydrogen or methane) volumetric and gravimetric capacities are given by Eqs. 1 and 2, using the usable mass of gas stored. Only the total and usable storage capacities will be presented and analyzed in this research.

## 2.3. Simulation Cells

The cells of the MOFs have been obtained from their files in the Crystallographic Information File (CIF) format on the CCDC database [26]. The set of 21 classical MOFs is composed by IRMOF-1 to IRMOF-20 (except 13, 17 and 19), HKUST-1, MOF-177, NU-111 and NU-125 (IRMOF: Isorecticular Metal-Organic Framework).

The MOF CCDC subset contains 106 Aluminum-based MOFs. The porosity and the density of the 106 were calculated. Among all of them, the ones with porosity above 40 % and density below 70 % were selected to make GCMC simulations and to compare their

GCMC storage capacities with those of the two novel MOFs. Usually, MOFs with those values of porosity and density have high storage capacities. This process led to a set of 15 selected Al-based MOFs whose CCDC database identifiers are: GUFYUE, MUZKEZ, OTECEX, OTEDOI, OTEDUO, OYEWEW, QOXQUS, QOXRAZ, QOXRIH, QOXSAA, QOXSUU, QOXTOP, QOXVEH, RIXPIZ and WOFQEQ.

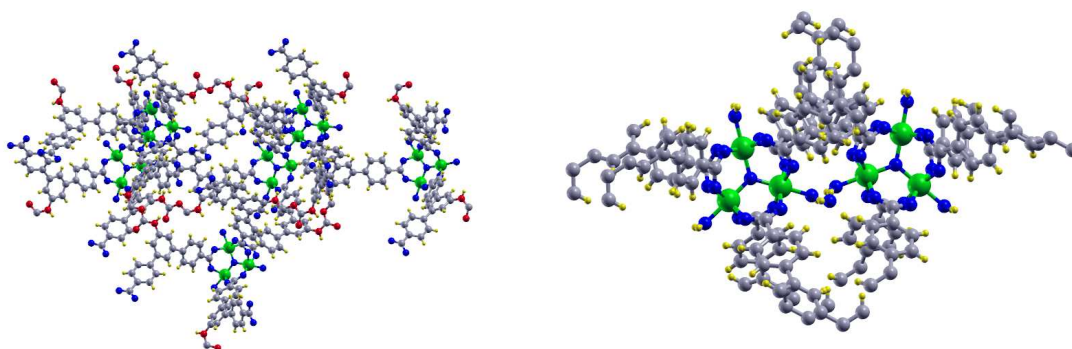


**Fig. 1.** Simulation cells of the two novel MOFs: Al-nia-MOF-1 and Al-nia-MOF-2 (left and right panels, respectively). Oxygen, carbon, hydrogen, aluminum and nitrogen atoms are represented by blue, gray, yellow, green and red balls, respectively.

### 3. Results

#### 3.1. Hydrogen Storage Capacities

Plots of the gravimetric and volumetric hydrogen storage capacities of Al-nia, the selected Al-based and classical MOFs as a function of density and porosity, at 298.15 K and 25 MPa, can be found in Fig. 2 and 3, respectively. It can be observed in those figures that the capacities are, in general, inversely proportional to the density and directly proportional to the porosity. This is a general trend: Some MOFs do not follow these trends. It can be also noticed in Fig. 2 that the gravimetric capacities of Al-nia MOFs lie approximately in the general line formed by the gravimetric capacities of classical and selected Al-based MOFs as a function of the density, i.e., their gravimetric capacities have the ‘expected’ gravimetric



capacity for their densities. In Fig. 3 Al-nia-MOFs present higher gravimetric capacity than classical and selected Al-based MOFs for similar porosities.

The selected Al-based MOFs have similar storage capacities, densities and porosities. Hence, in order to visualize correctly these points, specific plots of the capacities of this set of MOFs have been plotted and included in the lower panels of Fig. 2 and 3.

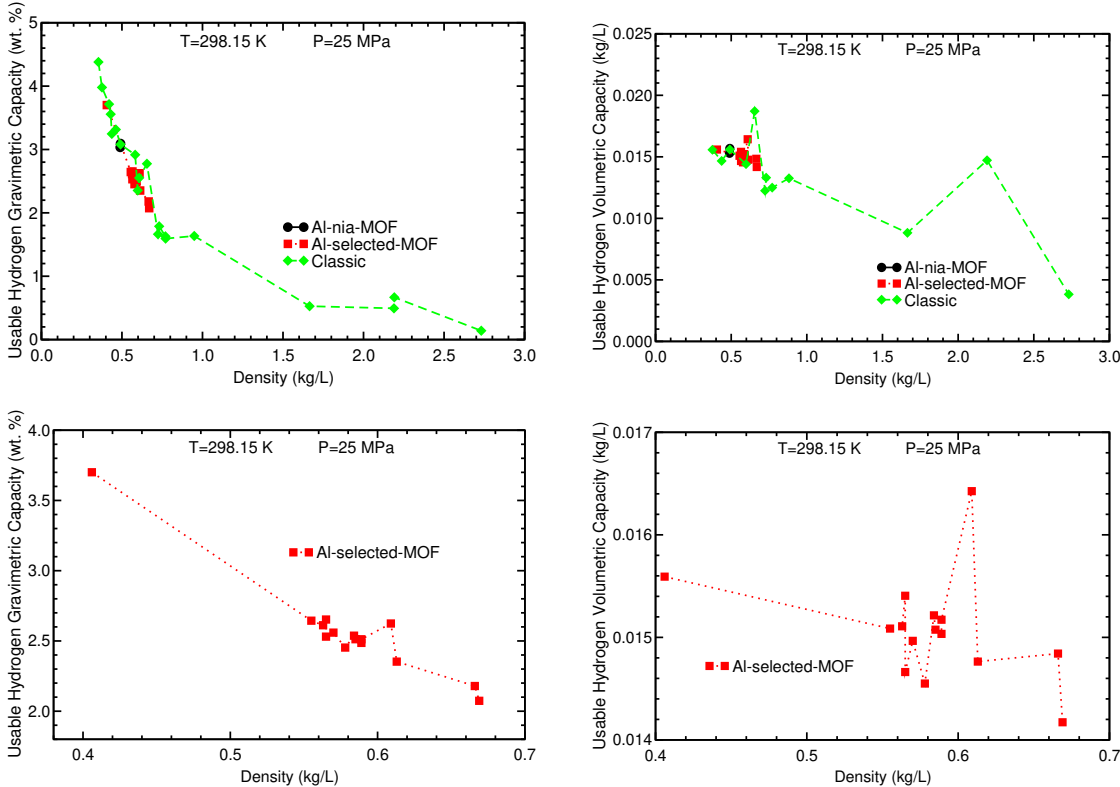


**Fig. 2.** Hydrogen gravimetric and volumetric usable capacity at 298.15 K and 25 MPa vs density of Al-nia, the selected Al-based and the classical MOFs. Low panels show a zoomed-in view of the capacities of the selected Al-based MOFs.

Hydrogen storage capacities of Al-nia-MOFs are very similar (See Table 3). At 298.15 K and 25 MPa gravimetric and volumetric usable capacities were found to be 3.03 wt. % and 0.015 kg/L for Al-nia-MOF-1, respectively. The gravimetric and volumetric usable capacities of Al-nia-MOF-2 are 3.09 wt. % and 0.016 kg/L, respectively. Porosity for Al-nia-MOF-1 and Al-nia-MOF-2 are 0.415 and 0.474, respectively. More porosity means higher gravimetric and volumetric usable capacities.

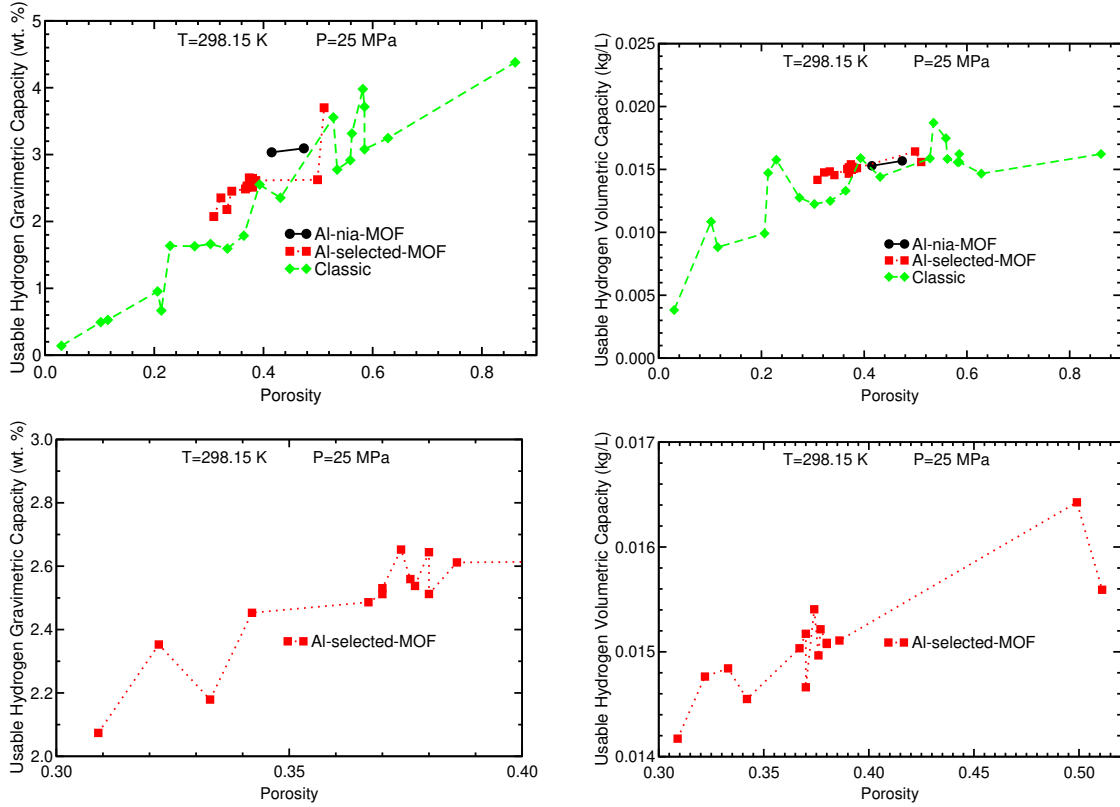


**Fig. 3.** Hydrogen gravimetric and volumetric usable capacity at 298.15 K and 25 MPa vs porosity of Al-nia, the selected Al-based and the classical MOFs. Low panels show a zoomed-in view of the capacities of the selected Al-based MOFs.

MOFs with the highest and the lowest gravimetric and volumetric capacities at 25 MPa of some selected Al-based and classical MOFs have been chosen to compare with the Al-nia-MOFs (See Table 3). Among selected Al-based MOFs, the one with the best volumetric capacity at 25 MPa, 0.016 kg/L, has the CCDC database identifier GUFYUE and the one with the best gravimetric capacity, 3.7 wt. %, is Al-soc-MOF-1 (CCDC database identifier MUZKEZ). This last MOF is reported as the current record holder for CO<sub>2</sub> storage [25, 47]. On the other hand, the MOF with the CCDC database identifier QOXTOP has the lowest gravimetric and volumetric capacities, 2.1 wt. % and 0.014 kg/L, respectively. Among the classical MOF collection, IRMOF-20 has the highest volumetric capacity (0.019 kg/L), IRMOF-15 has the highest gravimetric capacity, 4.4 wt. %. IRMOF-5 has the lowest gravimetric and volumetric capacities, 0.14 wt. % and 0.004 kg/L, respectively, of all the

Table 3: Hydrogen volumetric (in kg/L) and gravimetric (in wt. %) usable capacities at 298.15 K and 25 MPa obtained in the present GCMC simulations and density,  $\rho$ , (in kg/L) and porosity, prs., of the two novel Al-based MOFs, the selected Al-based and the classical MOFs.

MOF	$v_c$	$g_c$	$\rho$	prs.	MOF	$v_c$	$g_c$	$\rho$	prs.
Al-nia-MOF-1	0.0153	3.03	0.489	0.415	OYEWEW	0.0148	2.35	0.613	0.322
Al-nia-MOF-2	0.0157	3.09	0.491	0.474	QOXSA	0.0148	2.18	0.666	0.333
IRMOF-5	0.0038	0.14	2.731	0.030	OTEC	0.0152	2.51	0.589	0.370
IRMOF-8	0.0175	2.92	0.582	0.559	QOXQ	0.0150	2.49	0.589	0.367
IRMOF-12	0.0162	3.71	0.420	0.585	OTEDO	0.0151	2.51	0.585	0.380
IRMOF-14	0.0156	3.98	0.376	0.582	QOXVE	0.0152	2.54	0.584	0.377
IRMOF-15	0.0162	4.38	0.354	0.861	QOXSU	0.0146	2.45	0.578	0.342
IRMOF-20	0.0187	2.78	0.655	0.535	RIXPI	0.0150	2.56	0.570	0.376
MUZKEZ	0.0156	3.70	0.406	0.511	OTEDU	0.0147	2.53	0.565	0.370
GUFYUE	0.0164	2.62	0.609	0.499	WOFQE	0.0154	2.65	0.565	0.374
QOXTOP	0.0142	2.07	0.669	0.309	QOXRI	0.0151	2.61	0.563	0.386
					QOXRA	0.0151	2.64	0.555	0.380

MOFs in Table 3.

GCMC simulations of the H<sub>2</sub> storage capacities of MUZKEZ, GUFYUE, IRMOF-8, 12, 14, 15 and 20, and of the two novel Al-nia MOFs have been carried out at 298.15 K and pressures between 0.5 and 35 MPa. The gravimetric and volumetric usable capacities are compared on Fig. 4 and 5, as a function of the pressure. Gravimetric capacities are quite different. The gravimetric capacities of all these MOFs increase slowly and approximately linearly with the pressure. IRMOF-15 has the largest gravimetric capacity at any pressure and room temperature. MUZKEZ MOF gravimetric capacity is in between the gravimetric capacities of IRMOF-15 and Al-nia MOFs, which have lower values.

The volumetric capacities are very similar. Volumetric capacities for Al-nia, GUFYUE

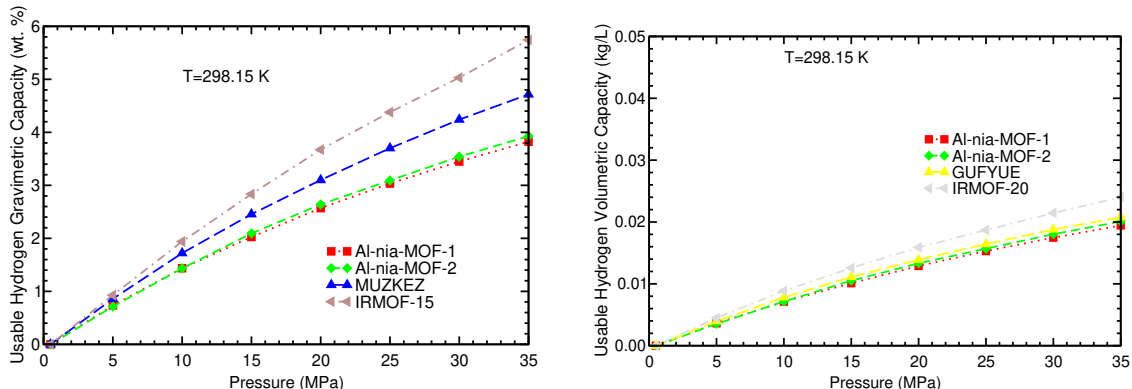


**Fig. 4.** Hydrogen volumetric and gravimetric usable capacities vs pressure at room temperature of some selected MOFs and the two novel Al-nia MOFs.

and QOXTOP MOFs are slightly smaller than the volumetric capacity of IRMOF-15 and IRMOF-20. The volumetric capacity of IRMOF-5 is much lower than the volumetric capacities of the other MOFs. From the highest to the lowest, the order is IRMOF-15, IRMOF-20, GUFYUE, Al-nia-MOF-2, Al-nia-MOF-1, QOXTOP and IRMOF-5.

The gravimetric storage capacities of the two novel Al-nia MOFs are high at 25-35 MPa, because their densities are low, below the water density, 1 kg/L. These MOFs are made of light elements (C, O, H and N) and of one of the lightest metals, Aluminum, and their structure is very porous (their hydrogen porosity is about 0.5). This explains their low density, below the water density, 1 kg/L, which, in turn, explains their high gravimetric storage capacities. As regards their volumetric storage capacities, they are high due to their high porosity, about 0.5.

With the aim of exploring the gravimetric and volumetric hydrogen storage capacities, a comparative study was carried out involving the two novel Al-nia-MOFs and a selection of the classical MOFs with the highest capacities: IRMOF-8, 12, 14, 15, and 20. GCMC simulations were performed at 298.15 K and pressures ranging from 0.5 to 35 MPa. The results of these simulations have been illustrated in Fig. 5.

The gravimetric capacities of the two Al-nia-MOFs, IRMOF-8 and 20 are very similar, while the gravimetric capacities of the other MOFs (IRMOF-12, 14 and 15) in Fig. 5 are about 20-50 % higher. This second group of MOFs has lower densities than the first group

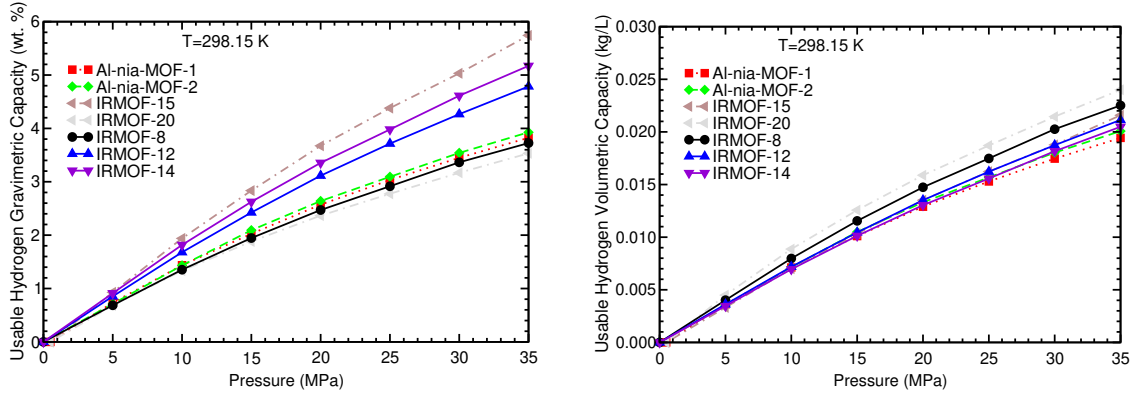


**Fig. 5.** Hydrogen volumetric and gravimetric usable capacities vs pressure at room temperature of some selected classical MOFs and the two novel Al-nia MOFs.

(See Table 3). This explains the higher gravimetric capacities of the second group of MOFs. The volumetric capacities of IRMOF-12, 14, and 15 and Al-nia-MOFs are very similar. The volumetric capacities of IRMOF-8 and 20 are slightly higher than the capacities of the other MOFs.

GCMC simulations of the hydrogen storage capacities of some MOFs with a different set of LJ coefficients, the MDT set, were carried out (See Table 2). The storage capacities at room temperature of Al-nia-MOFs and Al-nia-MOFs-MDT are compared in Fig. 6 as functions of pressure. Remarkably, the capacities of Al-nia-MOFs and Al-nia-MOFs-MDT display a high degree of similarity. The capacities of the Al-nia-MOFs-MDT are slightly higher than those of the Al-nia-MOFs. The differences between the capacities of Al-nia-MOF-1 and Al-nia-MOF-2 are almost identical to the differences between the capacities of Al-nia-MOF-1-MDT and Al-nia-MOF-2-MDT. The trend observed in the Al-nia-MOF-MDT curves closely resembled that of the Al-nia-MOF curves.

The storage capacities at 298.15 K of the best Al-based and classic MOFs with the original and MDT LJ sets are compared in Fig. 6 as functions of the pressure. The capacities obtained with these two LJ sets are, in general, similar. The capacities of IRMOF-15 and 20 obtained with the MDT LJ set are about 7-12 % higher than the capacities obtained with the original LJ set of coefficients. These differences between the results obtained with the two LJ sets are mainly due to the fact that the MDL LJ  $\epsilon$  coefficient of the hydrogen

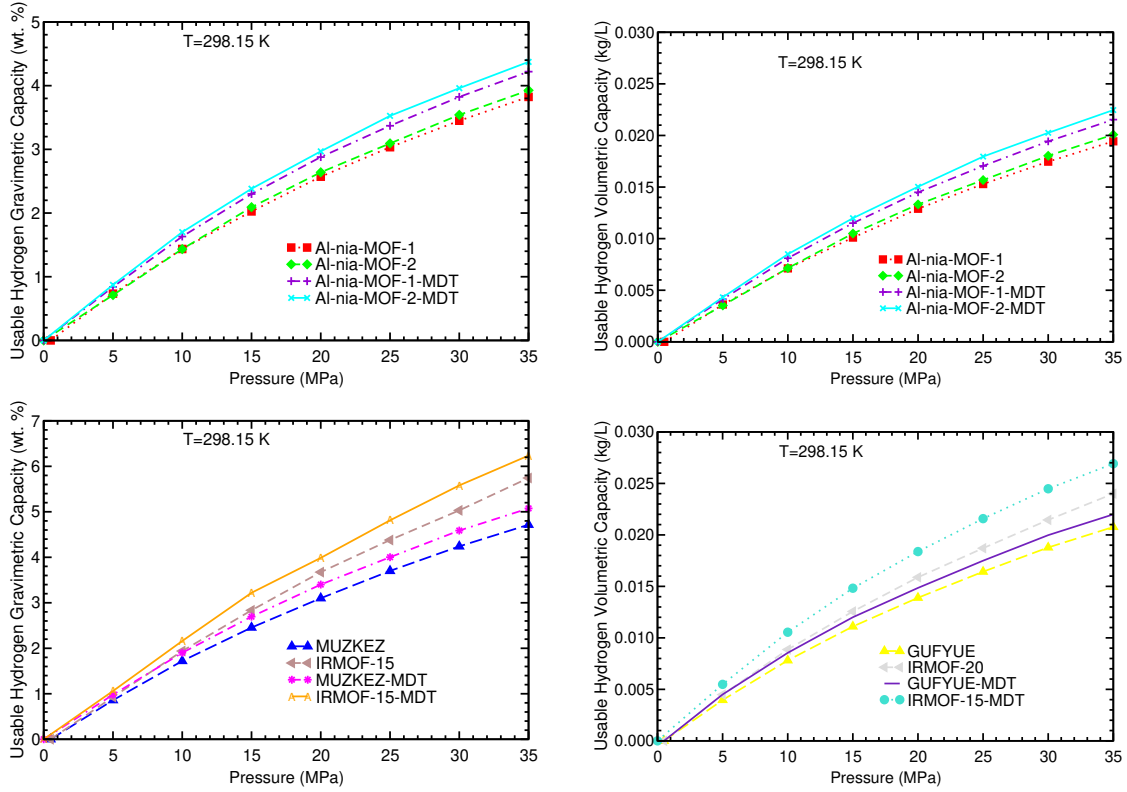


**Fig. 6.** Hydrogen gravimetric and volumetric usable capacity vs pressure at room temperature of the Al-nia-MOFs (upper panels) and the best Al-based MOF, MUZKEZ, and the best classical MOF for gravimetric, IRMOF-15, and for volumetric capacity, IRMOF-20 (lower panels).

molecule, 0.003163 eV, is slightly larger than the counterpart in the original LJ set, 0.002870 eV (See Tables 1 and 2).

### 3.2. Methane Storage Capacities

The methane storage capacities have been also investigated. The two novel Al-nia MOFs have similar methane storage capacities. At 298.15 K and 25 MPa the usable methane gravimetric and volumetric capacities were found to be, respectively, 27.2 wt. % and 0.183 kg/L for Al-nia-MOF-1, and 28.1 wt. % and 0.192 kg/L for the Al-nia-MOF-2. These capacities are high and very close to the DOE methane targets.

The methane storage capacities of Al-nia, some selected Al-based and classical MOFs, at 298.15 and 25 MPa, as functions of density and porosity have been plotted in Fig. 7 and 8, respectively. The methane storage capacities, densities and porosities of the selected

Al-based MOFs are similar and therefore, to visualize them correctly, the results of these MOFs have been represented in the lower panels of those figures. The storage capacities are, in general, inversely proportional to the density and directly proportional to the porosity. The gravimetric methane capacities of the two novel Al-nia MOFs lie approximately in the general line formed by the gravimetric capacities of classical and selected Al-based MOFs as a function of the density. The methane and hydrogen storage capacities share these same trends or dependences on the density and porosity.

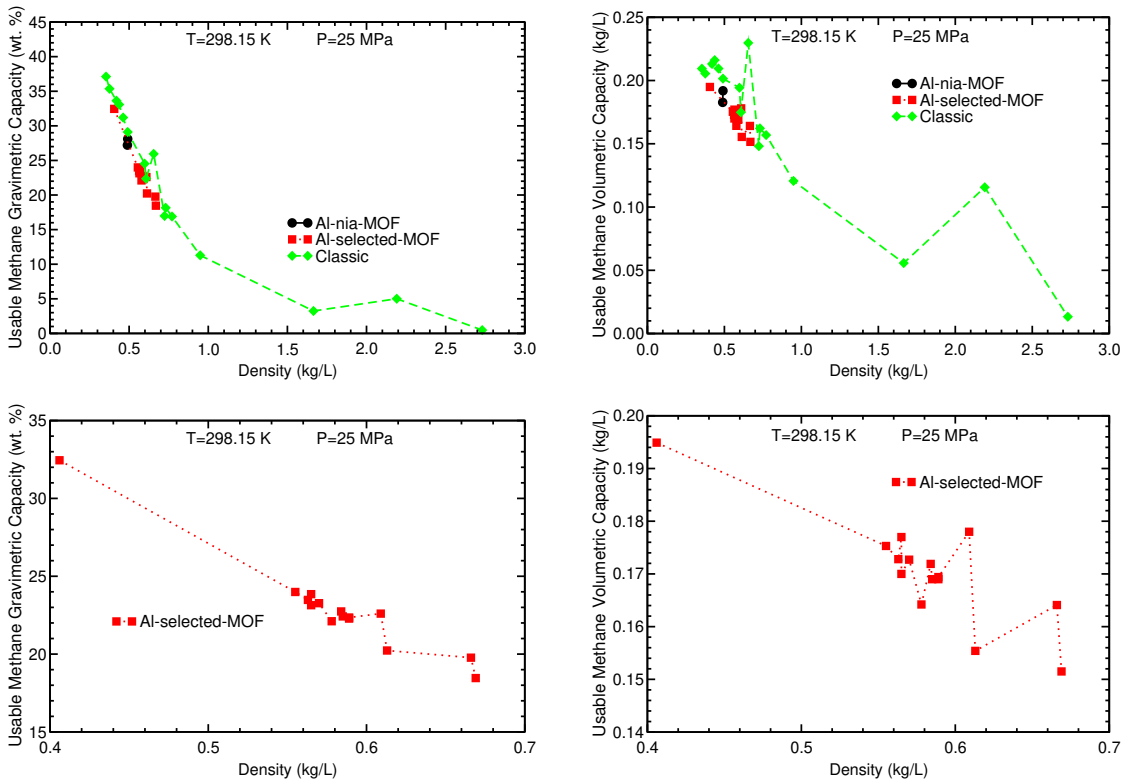


**Fig. 7.** Methane gravimetric and volumetric usable capacity at 298.15 K and 25 MPa vs density of Al-nia, the selected Al-based and the classical MOFs. Low panels show a zoomed-in view of the selected Al-based MOFs.

As it was done for hydrogen storage, MOFs with the highest gravimetric and volumetric methane storage capacities at 25 MPa from the selected Al-based and the classical MOFs were chosen (See Table 4) to make GCMC simulations between 0.5 and 35 MPa. Among the selected Al-based MOFs, the one with the best methane volumetric and gravimetric

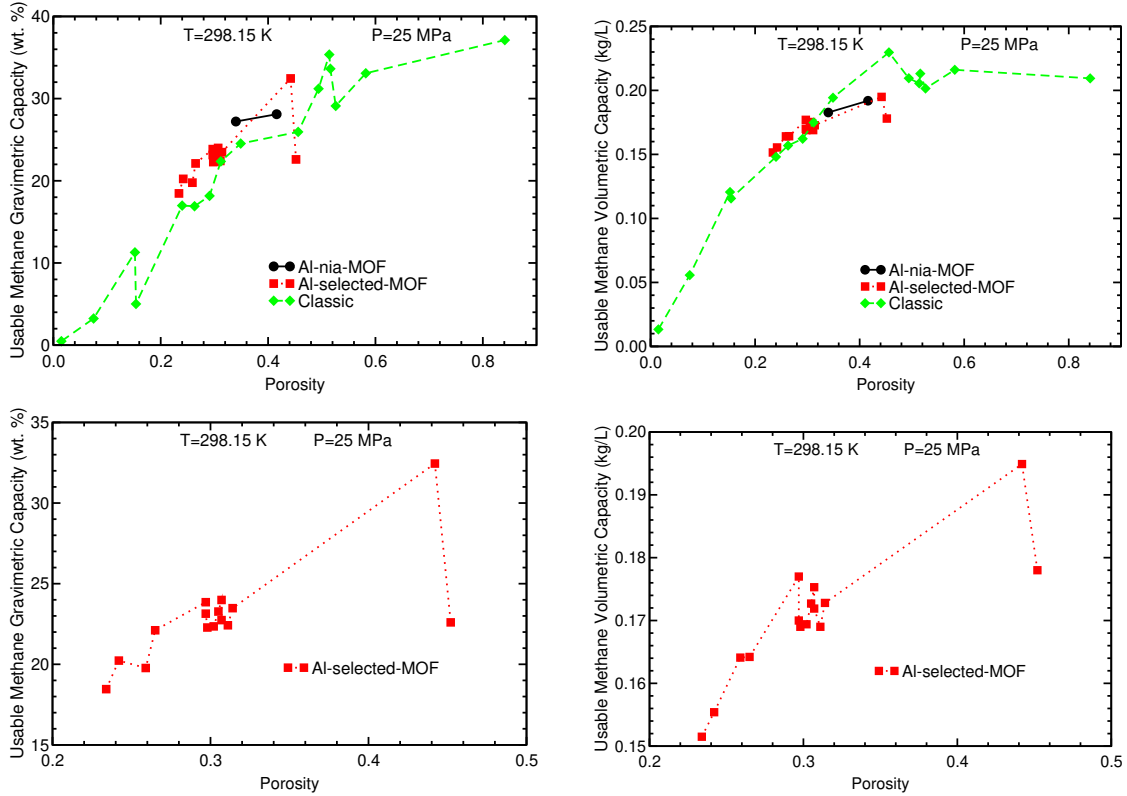


**Fig. 8.** Methane gravimetric and volumetric usable capacity at 298.15 K and 25 MPa vs porosity of Al-nia, the selected Al-based and the classical MOFs. Low panels show a zoomed-in view of the selected Al-based MOFs.

capacities, 0.195 kg/L and 32.5 wt. %, is named MUZKEZ, and it is also one of the selected Al-based MOFs of the CCDC database with the best hydrogen gravimetric capacity. The one with the lowest methane volumetric and gravimetric capacities, 0.151 kg/L and 18.5 wt. %, respectively, is QOXTOP, again in agreement with the hydrogen capacities results.

Among the classical MOF set, IRMOF-20 has the highest volumetric capacity, 0.230 kg/L, and IRMOF-15 has the highest gravimetric capacity, 37.1 wt. %. The lowest gravimetric capacities correspond to QOXTOP MOF, among selected Al-based MOFs, and to IRMOF-5, among the classical MOF collection. All these results are also in agreement with the results obtained for the hydrogen case.

The usable methane gravimetric and volumetric capacities of selected Al-based, classical MOFs and Al-nia MOFs are compared on Fig. 9 and 10, as functions of the pressure in



Table 4: Methane volumetric (in kg/L) and gravimetric (in wt. %) usable capacities at 298.15 K and 25 MPa obtained in the present GCMC simulations and density,  $\rho$ , (in kg/L) and porosity (prs.) of the two novel Al-based MOFs, the selected Al-based and the classical MOFs.

MOF	$v_c$	$g_c$	$\rho$	prs.	MOF	$v_c$	$g_c$	$\rho$	prs.
Al-nia-MOF-1	0.183	27.2	0.489	0.340	OYEWEW	0.155	20.2	0.613	0.242
Al-nia-MOF-2	0.192	28.1	0.491	0.416	QOXSA	0.164	19.8	0.666	0.259
IRMOF-5	0.013	0.5	2.731	0.015	OTECEX	0.169	22.4	0.589	0.302
IRMOF-8	0.223	27.7	0.582	0.491	QOXQUS	0.169	22.3	0.589	0.298
IRMOF-12	0.213	33.6	0.420	0.516	OTEDO	0.169	22.4	0.585	0.311
IRMOF-14	0.206	35.4	0.376	0.514	QOXVEH	0.172	22.7	0.584	0.307
IRMOF-15	0.209	37.1	0.354	0.841	QOXSUU	0.164	22.1	0.578	0.265
IRMOF-20	0.230	26.0	0.655	0.456	RIXPIZ	0.173	23.3	0.570	0.305
MUZKEZ	0.195	32.5	0.406	0.442	OTEDUO	0.170	23.1	0.565	0.297
GUFYUE	0.178	22.6	0.609	0.452	WOFQEQ	0.177	23.9	0.565	0.297
QOXTOP	0.151	18.5	0.669	0.234	QOXRIH	0.173	23.5	0.563	0.314
					QOXRAZ	0.175	24.0	0.555	0.307

a range between 0.5 and 35 MPa. Usable gravimetric capacities are quite different. The gravimetric storage of all the MOFs increase very fast at low pressures and all of them start to saturate approximately at 10 MPa. IRMOF-15 has the largest gravimetric capacity from 8 MPa, approximately, and at room temperature. Al-nia MOFs, IRMOF-15 and MUZKEZ have similar gravimetric capacities in the pressure interval of 0.5-8 MPa, but Al-nia-MOF-2 has the highest one. MUZKEZ MOF gravimetric capacity is approximately in the middle, between the IRMOF-15 and Al-nia MOFs capacities, which have lower values. Al-nia MOFs do not reach the DOE targets for methane, but they are very close. IRMOF-15 reaches the gravimetric target when pressure gets to 16 MPa and MUZKEZ when it reaches 30 MPa. On the other hand, volumetric capacities are very similar. The volumetric capacities for

Al-nia and MUZKEZ MOFs are slightly smaller than the volumetric capacity of IRMOF-20.

The methane storage capacities of the two novel Al-nia MOFs are high at 25-35 MPa and are close to the capacities of the best classical and Al-based MOFs. This is due to their low density and high porosity (See Fig. 9 and Table 4).

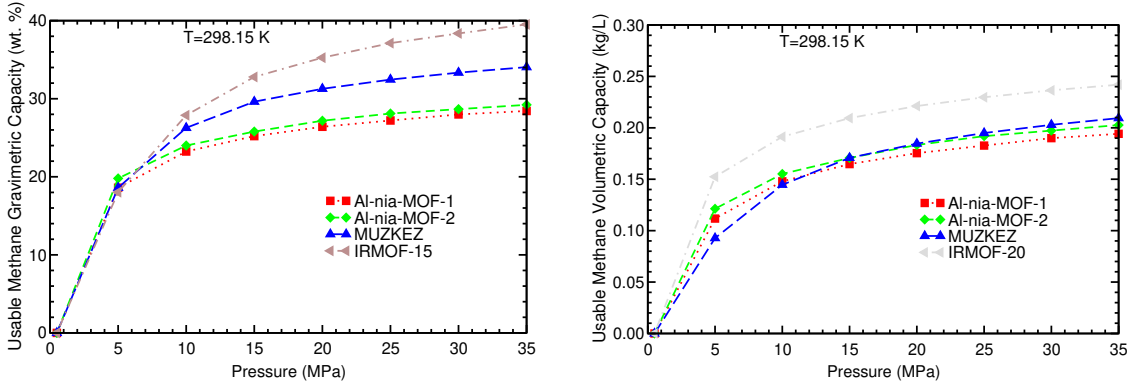


**Fig. 9.** Methane volumetric and gravimetric usable capacities vs pressure at room temperature of some selected MOFs and the two novel Al-nia MOFs.

A comparison of the storage capacities of the Al-nia-MOFs and the classical MOFs with the highest methane storage capacities at 25 MPa: IRMOF-8, 12, 14, 15, and 20, was also carried out and is depicted in Fig. 10. The gravimetric capacities of the two Al-nia-MOFs, IRMOF-8 and IRMOF-20 are relatively similar and smaller than the capacities of the other MOFs. The volumetric capacities of the classical MOFs are very similar and higher than the volumetric capacities of the Al-nia-MOFs.

Similar to the hydrogen case, simulations have been conducted to calculate the methane storage capacities with the MDT set of LJ coefficients (See Table 2). The resulting storage capacities at room temperature have been depicted in Fig. 11 as functions of pressure. Remarkably, both Al-nia-MOFs and Al-nia-MOFs-MDT showcase almost identical capacities. The same applies to the best selected Al-based MOFs and classical MOFs studied (MUZKEZ, GUFYUE, IRMOF-15 and IRMOF-20). This close similarity is mainly due to the nearly identical LJ coefficients of the methane molecule (See Tables 1 and 2).

Alezi et al. [25] have found that Al-nia-MOF-1 has a slightly higher porosity than Al-nia-MOF-2 [25], in contrast with the present GCMC simulations: Al-nia-MOF-2 presents a

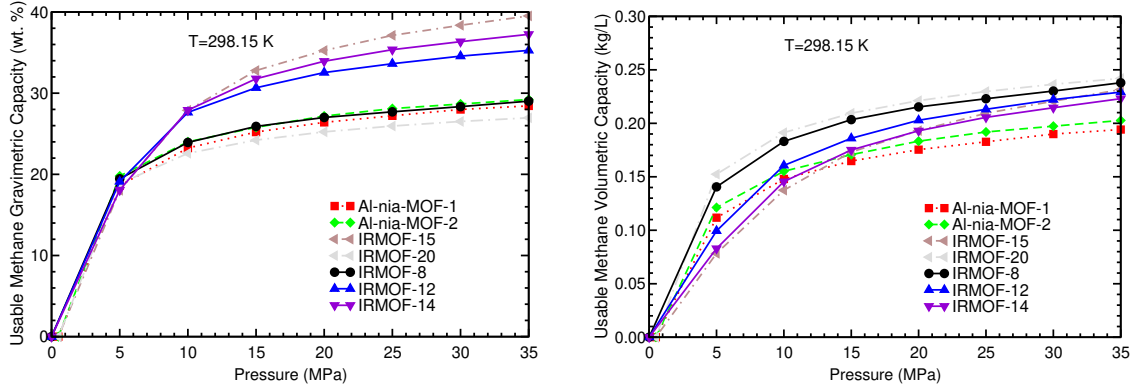


**Fig. 10.** Methane volumetric and gravimetric usable capacities at room temperature vs pressure of some selected classical MOFs and the two novel Al-nia-MOFs.

slightly higher porosity than Al-nia-MOF-1, 0.416 and 0.340 for methane, respectively (See Table 4). Alezi et al. [25] investigated  $\text{CH}_4$  adsorption on Al-nia-MOF-1 at 8 MPa and different temperatures. The storage capacities obtained by Alezi et al. and the theoretical capacities obtained in the present GCMC simulations are shown and compared in Table 5.

The theoretical GCMC and experimental volumetric and gravimetric storage capacities are quite similar. The theoretical capacities are about 6-14 % higher than the experimental ones. On the other hand, the theoretical capacities from the MDT set are very similar to the theoretical capacities obtained using the original set of LJ values and slightly closer to the experimental results. The difference between the values of  $\sigma$  and  $\epsilon$  for methane of the two sets of LJ values is very small and this causes, in turn, small differences between the methane capacities obtained using the two sets of LJ values. The usable capacities reported by Alezi et al. [25] are estimated, not measured values. This comparison with the experiments is very relevant and allow us to estimate the relative error of the present GCMC predictions of the storage capacities.

The GCMC simulations are based on the experimental MOF structure and hence, on the crystal density, but the density of the samples of MOFs used in the experiments is the packing density, which is usually larger than the crystal density. The smaller crystal density implies that the theoretical storage capacities are larger than the experimental storage capacities.

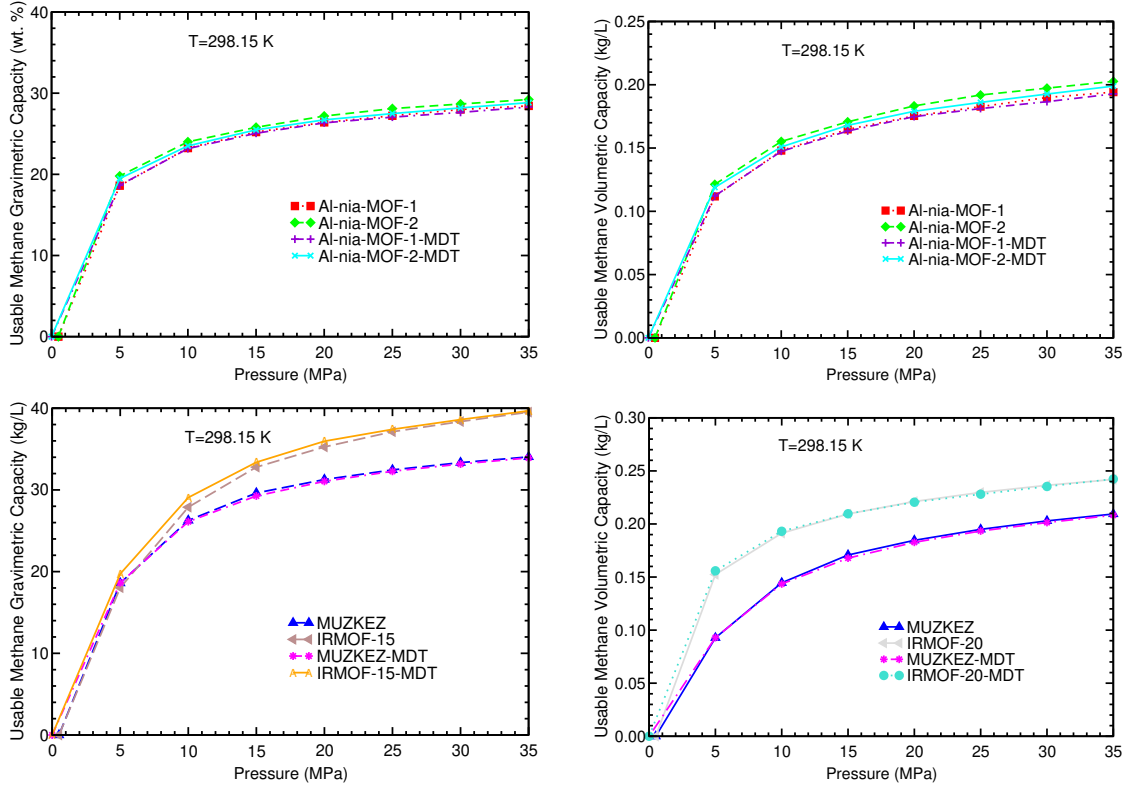


**Fig. 11.** Methane gravimetric and volumetric usable capacity vs pressure at room temperature of the Al-nia-MOFs (upper panels) and the best Al-based MOF, MUZKEZ, and the best classical MOF for gravimetric, IRMOF-15, and for volumetric capacity, IRMOF-20 (lower panels).

#### 4. Conclusions and future lines

The present GCMC results are predictions of the usable hydrogen and methane storage capacities of two novel Al-nia MOFs, Al-nia-MOF-1 and Al-nia-MOF-2, at room temperature and pressures between 0.5 and 35 MPa, and they could be useful for experimentalists.

According to the present GCMC simulations, the two novel Al-nia MOFs show high hydrogen and methane storage capacities at room temperature and pressures of 25-35 MPa, comparable to those of the best classical and Al-based MOFs. The usable hydrogen storage capacities of these two MOFs are about 3 wt. % and 0.016 kg/L and their usable methane storage capacities are about 28 wt. % and 0.190 kg/L at room temperature and 25-35 MPa.

The methane storage capacities of Al-nia-MOF-1 obtained in the GCMC simulations at room temperatures (258, 273 and 298 K) and 8 MPa are very similar to the experimental

Table 5: Experimental and present GCMC total and usable methane storage capacities of Al-nia-MOF-1. Pressure is in MPa, temperatures are in K,  $v_c$  in kg/L and  $g_c$  in wt. % units. The experimental results have been published by Alezi et al. [25].

P	T	$v_c$	$g_c$	Capacities	Source
8	258	0.188	28.6	Total	Experiments
8	258	0.201	29.1	Total	GCMC
8	258	0.199	28.9	Total	GCMC MDT
8	273	0.166	24.5	Total	Experiments
8	273	0.187	27.6	Total	GCMC
8	273	0.182	27.2	Total	GCMC MDT
8	298	0.142	23.1	Total	Experiments
8	298	0.161	24.8	Total	GCMC
8	298	0.159	24.5	Total	GCMC MDT
8	298	0.123	21.3	Usable	Experiments
8	298	0.139	22.1	Usable	GCMC
8	298	0.138	22.0	Usable	GCMC MDT

values at the same temperatures and pressure reported by Alezi et al. [25]. The obtained GCMC methane storage capacities are about 6-14 % higher than the experimental values.

The dependence of the hydrogen volumetric and gravimetric storage capacities of the MOFs studied (classical, Al-based and the two novel MOFs) on the porosity and density has been studied. The analysis reveals that the capacities are inversely proportional to the density and proportional to the porosity. The origin of the high capacities of the novel MOFs are their high porosity and low density and these capacities could be improved by doping these novel MOFs with some light elements.

**Acknowledgment** This work was founded by MICINN research project from Spain (Grant PGC2018-093745-B-I00), Junta de Castilla y León (Grant VA124G18) and the Uni-

versity of Valladolid, Spain. The use of the computer facilities of Centro de Proceso de Datos - Parque Científico of the University of Valladolid is acknowledged.

## References

- [1] Breeze, P.. Hydrogen energy storage. In: Power system energy storage technologies; chap. 8. London: Elsevier; 2018, p. 69–77.
- [2] Allendorf, M.D., Hulvey, Z., Gennett, T., Ahmed, A., Autrey, T., Camp, J., et al. An assessment of strategies for the development of solid-state adsorbents for vehicular hydrogen storage. *Energy Environ Sci* 2018;11:2784–2812. doi:10.1039/C8EE01085D.
- [3] Office of Energy Efficiency & Renewable Energy, Fuel Cell Technologies Office. DOE technical targets for onboard hydrogen storage for light-duty vehicles. <https://www.energy.gov/eere/fuelcells/doe-technical-targets-onboard-hydrogen-storage-light-duty-vehicles>; 2018. Accessed July 14, 2023.
- [4] Yang, Q., Guillerm, V., Ragon, F., Wiersum, A.D., Llewellyn, P.L., Zhong, C., et al. CH<sub>4</sub> storage and CO<sub>2</sub> capture in highly porous zirconium oxide based metal–organic frameworks. *Chem Commun* 2012;48:9831–9833. doi:10.1039/C2CC34714H.
- [5] Advanced Research Projects Agency - Energy, DOE. Methane Opportunities for Vehicular Energy (MOVE) Program Overview. [http://arpa-e.energy.gov/sites/default/files/documents/files/MOVE\\_ProgramOverview.pdf](http://arpa-e.energy.gov/sites/default/files/documents/files/MOVE_ProgramOverview.pdf); 2012. Accessed July 14, 2023.
- [6] International Organization for Standardization. ISO 15403-1:2006(en) Natural gas — Natural gas for use as a compressed fuel for vehicles — Part 1: Designation of the quality. <https://www.iso.org/obp/ui/#iso:std:44211:en>; 2006. Accessed July 14, 2023.
- [7] Office of Energy Efficiency & Renewable Energy, Hydrogen and Fuel Cell Technologies Office. High-Pressure Hydrogen Tank Testing. <https://www.energy.gov/eere/fuelcells/high-pressure-hydrogen-tank-testing>; 2022. Accessed July 14, 2023.
- [8] Zhang, H., Zheng, Y., Cui, Y.. Melamine assisted preparation of nitrogen doped activated carbon from sustainable biomass for h<sub>2</sub> and co<sub>2</sub> storage. *Int J Hydrogen Energy* 2023;48:17914–17922. doi:10.1016/j.ijhydene.2023.01.269.
- [9] Alali, I., Mokaya, R.. Direct synthesis of organic salt-derived porous carbons for enhanced CO<sub>2</sub> and methane storage. *J Mater Chem A* 2023;11:6952–6965. doi:10.1039/D3TA00044C.
- [10] Blankenship, L.S., Mokaya, R.. Modulating the porosity of carbons for improved adsorption of hydrogen, carbon dioxide, and methane: a review. *Mater Adv* 2022;3:1905. doi:10.1039/d1ma00911g.
- [11] Attia, N.F., Jung, M., Park, J., Cho, S.Y., Oh, H.. Facile synthesis of hybrid porous composites and its porous carbon for enhanced H<sub>2</sub> and CH<sub>4</sub> storage. *Int J Hydrogen Energy* 2020;45:32797–32807.

- [12] Vos, J.S.D., Borgmans, S., Voort, P.V.D., Rogge, S.M.J., Speybroeck, V.V.. ReDD-COFFEE: a ready-to-use database of covalent organic framework structures and accurate force fields to enable high-throughput screenings. *J Mater Chem A* 2023;11:7468–7487. doi:10.1039/d3ta00470h.
- [13] Dong, Y., Zhang, X., Wang, Y., Tang, L., Yang, Y.. Engineering building blocks of covalent organic frameworks for boosting capacitive charge storage. *J Power Sources* 2023;564:232873. doi:10.1016/j.jpowsour.2023.232873.
- [14] Wang, Z., Li, X.M., Li, H.. Stable and microporous covalent organic frameworks via weak interactions for gas uptake. *CrystEngComm* 2023;25:1910–1914. doi:10.1039/D2CE01645A.
- [15] Morgan, W.J., Anstine, D.M., Colina, C.M.. Temperature effects in flexible adsorption processes for amorphous microporous polymers. *J Phys Chem B* 2022;126:6354–6365. doi:10.1021/acs.jpcc.2c04543.
- [16] Chen, Z., Kirlikovali, K.O., Idrees, K.B., Wasson, M.C., Farha, O.K.. Porous materials for hydrogen storage. *Chem* 2022;8:693–716. doi:10.1016/j.chempr.2022.01.012.
- [17] Tian, M., Rochat, S., Fawcett, H., Burrows, A.D., Bowen, C.R., Mays, T.J.. Chemical modification of the polymer of intrinsic microporosity PIM-1 for enhanced hydrogen storage. *Adsorption* 2020;26:1083–1091. doi:10.1007/s10450-020-00239-y.
- [18] Lu, X., Tang, Y., Yang, G., Wang, Y.Y.. Porous functional metal-organic frameworks (mofs) constructed from different n-heterocyclic carboxylic ligands for gas adsorption/separation. *CrystEngComm* 2023;25:896–908. doi:10.1039/d2ce01667b.
- [19] Liu, Y., Shen, D., Tu, Z., Xing, L., Chung, Y.G., Li, S.. Room-temperature hydrogen storage performance of metal-organic framework/graphene oxide composites by molecular simulations. *Int J Hydrogen Energy* 2022;47:41055–41068.
- [20] Li, A.. Metal-organic frameworks-based hydrogen storage strategies and applications. *J Phys: Conf Ser* 2022;2403(1):012022. doi:10.1088/1742-6596/2403/1/012022.
- [21] Shet, S.P., Priya, S.S., Sudhakar, K., Tahir, M.. A review on current trends in potential use of metal-organic framework for hydrogen storage. *Int J Hydrogen Energy* 2021;46:11782–11803. doi:10.1016/j.ijhydene.2021.01.020.
- [22] Yu, S., Jing, G., Li, S., Li, Z., Ju, X.. Tuning the hydrogen storage properties of MOF-650: A combined DFT and GCMC simulations study. *Int J Hydrogen Energy* 2020;45:6757–6764.
- [23] Cabria, I., Suárez-García, F., Mazadiego, L.F., Ortega, M.F.. Methane storage in nanoporous carbons. In: *21st Century Nanoscience – A Handbook: Low-Dimensional Materials and Morphologies*, Volume 4; chap. 23. Boca Raton: CRC Press; 2020, p. 1–14. doi:10.1201/9780429347290.
- [24] Yabing, H., Zhou, W., Guodong, Q., Chen, B.. Methane storage in metal-organic frameworks. *Chem Soc Rev* 2014;45:5657–5678.

- [25] Alezi, D., Jia, J., Bhatt, P.M., Shkurenko, A., Solovyeva, V., Chen, Z., et al. Reticular chemistry for the construction of highly porous aluminum-based nia-metal-organic frameworks. *Inorganic Chemistry* 2022;61(28):10661–10666. doi:10.1021/acs.inorgchem.2c00756.
- [26] Cambridge Crystallographic Database Centre. [www.ccdc.cam.ac.uk](http://www.ccdc.cam.ac.uk); 2023. Accessed July 14, 2023.
- [27] Metropolis, N.. The Beginning of the Monte Carlo Method. *Los Alamos Science* 1987;15:125–130.
- [28] Soave, G.. Equilibrium constants from a modified Redlich-Kwong equation of state. *Chem Eng Sci* 1972;27:1197–1203.
- [29] Zhou, L., Zhou, Y.. Determination of compressibility factor and fugacity coefficient of hydrogen in studies of adsorptive storage. *Int J Hydrogen Energy* 2001;26:597–601.
- [30] Xu, X.H., Duan, Y.Y., Yang, Z.. Crossover volume translation Soave-Redlich-Kwong equation of state for fluids. *Ind Eng Chem Res* 2012;51:6580–6585.
- [31] Lennard-Jones, J.E.. On the determination of molecular fields. *Proc Roy Soc (London) A* 1924;106:463–477. doi:10.1098/rspa.1924.0082.
- [32] Filippova, V.P., Kunavin, S.A., Pugachev, M.S.. Calculation of the parameters of the Lennard-Jones potential for pairs of identical atoms based on the properties of solid substances. *Inorganic Materials: Applied Research* 2015;6:1–4.
- [33] Mayo, S.L., Olafson, B.D., Goddard III, W.A.. DREIDING: A generic force field. *J Phys C: Solid State Phys* 1990;94:8897–8909.
- [34] Tu, Y., Xiu, P., Wan, R., Hu, J., Zhou, R., Fang, H.. Water-mediated signal multiplication with Y-shaped carbon nanotubes. *Proc Natl Acad Sci USA* 2009;106:18120–18124.
- [35] Singer, K., Taylor, A., Singer, J.V.L.. Thermodynamic and structural properties of liquids modelled by ‘2-Lennard-Jones centres’ pair potentials. *Mol Phys* 1977;33:1757–1795. doi:10.1080/00268977700101451.
- [36] Cheung, P.S.Y., Powles, J.G.. The properties of liquid nitrogen. *Mol Phys* 1975;30:921–949.
- [37] Soper, A.K.. The structure of molten  $\text{ZnCl}_2$ : A new analysis of some old data. *Pramana Journal of Physics* 2004;63:41–50.
- [38] Rzepka, M., Lamp, P., de la Casa-Lillo, M.A.. Physisorption of hydrogen on microporous carbon nanotubes. *J Phys Chem B* 1998;102:10894–8.
- [39] Jorgensen, W.L., Madura, J.D., Swenson, C.J.. Optimized intermolecular potential functions for liquid hydrocarbons. *J Am Chem Soc* 1984;106:6638–6646.
- [40] Good, R.J., Hope, C.J.. New combining rule for intermolecular distances in intermolecular potential functions. *J Chem Phys* 1970;53:540–543. doi:10.1063/1.1674022.
- [41] Berthelot, D.. Sur le mélange des gaz. *Comptes rendus hebdomadaires des séances de l’Académie des Sciences* 1898;126:1703.



- [42] Feynman, R.P., Hibbs, A.. Quantum Mechanics and Path Integrals. New York: McGraw-Hill; 1965.
- [43] Darkrim, F., Levesque, D.. Monte Carlo simulations of hydrogen adsorption in single-walled carbon nanotubes. *J Chem Phys* 1998;109:4981–4984.
- [44] Transferable Potentials for Phase Equilibria. TraPPE-United Atom. <http://trappe.oit.umn.edu/#UA>; 2023. Accessed July 14, 2023.
- [45] Broom, D.P., Webb, C.J., Fanourgakis, G.S., Froudakis, G.E., Trikalitis, P.N., Hirscher, M.. Concepts for improving hydrogen storage in nanoporous materials. *Int J Hydrogen Energy* 2019;44:7768–7779.
- [46] Schlichtenmayer, M., Hirscher, M.. The usable capacity of porous materials for hydrogen storage. *Appl Physics A* 2016;122:379. doi:10.1007/s00339-016-9864-6.
- [47] Alezi, D., Belmabkhout, Y., Suyetin, M., Bhatt, P.M., Weseliński, L.J., Solovyeva, V., et al. MOF crystal chemistry paving the way to gas storage needs: Aluminum-based soc-MOF for CH<sub>4</sub>, O<sub>2</sub>, and CO<sub>2</sub> storage. *J Am Chem Soc* 2015;137(41):13308–13318. doi:10.1021/jacs.5b07053.